JOURNAL OF APPLIED ELECTROCHEMISTRY 19 (1989) 90–94

Estimation of optimum anode geometry in chlor-alkali membrane cells

Y. NISHIKI, S. NAKAMATSU

Research and Development Centre, Permelec Electrode Ltd, 1159 Ishikawa, Fujisawa 252, Japan

K. AOKI, K. TOKUDA

Department of Electronic Chemistry, Graduate School at Nagatsuta, Tokyo Institute of Technology, Nagatsuta, Midori-ku, Yokohama 227, Japan

Received 18 March 1988; revised 8 June 1988

In order to explore the dependence of cell voltage on electrode geometries, precious metal oxide anodes (DSA®) with the following three kinds of geometries were constructed: an assembled strip with a parallel array (louvre type), a circularly perforated plate and a flattened mesh. Voltages in the membrane cell of a laboratory scale were measured with chlorine gas evolution in NaCl solution. The cell voltages exhibited a linear relation to a unit cell characteristic dimension as well as to the square of the per cent open area of the anode, as predicted from the theoretical analysis of the primary current distribution in the two-dimensional rectangular model cell. Therefore, small sizes of the iterative pattern unit reduced cell voltages. Slopes of the linear relation gave the increase in solution resistivity caused by the gas bubbles, indicating the presence of a bubble curtain around the anode.

Nomenclature

d_1	distance between the anode and the membrane
d_2	thickness of the membrane
j	averaged current density, i.e. the current divided by (width of the anode) × (height of the anode)
o_p	per cent open area defined by Equation 2
p	pitch of the unit region
p_{cp}	pitch of the unit region for the circularly perforated anode
p_L	pitch of the unit region for the louvered anode
p_{LW}, p_{SW}	pitch of the unit region for the mesh anode (see Fig. 2c)
r	radius of the circular open part
V	cell voltage of the whole cell
V_{rs}	residual voltage, i.e. the sum of the voltages such as overpotential due to electrode kinetics both at the anode and the cathode, ohmic drop in the catholyte, membrane potential drop and ohmic drop within both electrodes
ϱ_{bc}	apparent resistivity of the anolyte containing gas bubbles
ϱ_2	resistivity of the membrane
θ	arctan (p_{SW}/p_{LW})

1. Introduction

Electrode geometry is one of the important factors which determine the performance of a cell with gas-evolving electrodes such as chlor-alkali membrane cells. Gas bubbles evolving in these cells need to be removed rapidly from the interelectrode gap in order to reduce cell voltage and to restore the active electrode surface. A technique of rapid removal of gas bubbles is to make voids or holes for gas passage in the electrode. In order to promote gas removal, several types of electrode geometry, e.g. a flattened mesh, a louvre type, a perforated plate and a woven electrode, have been designed. As a model of these electrodes, a two-dimensional rectangular model electrode with an open part has been introduced [1], and current distribution and cell resistance have been evaluated theoretically for the cases of both the primary [1] and secondary [2] current distributions, and for electrode reactions in the two-dimensional two-layer model cell composed of a bubble curtain and a convective layer [3]. Investigation of electrode geometries with open parts may involve such subjects as dependence of cell voltage and current distribution on a per cent open area [1–14], on sizes of an iterative unit with an open part [1, 3], on electrode resistance [4, 11, 12, 14] and on the dimensions and scale of a whole cell. Although the first two subjects have been dealt with theoretically in previously papers [1–3], there have been few reports [5] concerning the variations of cell voltage with the per cent open area and sizes of iterative units or meshes on the basis of data measured at electrodes employed for industrial electrolysis. In this report, cell voltages in a laboratory-scale cell were measured at electrodes with various kinds of geometry and were compared with the theoretical estimation.

0021-891X/89 $03.00 + .12

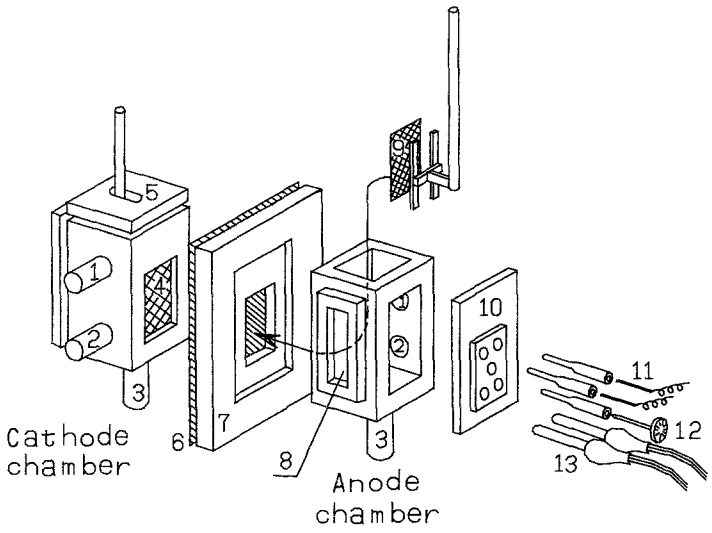

Fig. 1. Schematic diagram of the electrochemical cell. (1) Solution outlet; (2) solution inlet; (3) drain; (4) cathode; (5) top lid; (6) ion exchange membrane; (7) membrane holder; (8) sight glass; (9) anode; (10) back lid; (11) thermosensor; (12) thermometer; (13) heater.

2. Experimental details

A two-compartment laboratory scale cell made of Teflon was 10 × 12 × 20 (height) cm^3 in size and 1000 cm^3 in solution capacity, as illustrated in Fig. 1. Anolyte and catholyte were separated by an ion-exchange membrane, Nafion® 901. The membrane was mechanically pressed onto an anode surface by a pressure difference between the two compartments. A Ni cathode of a mesh type was mounted 2 mm from the membrane. The compartment for the anolyte had an opening with a lid, through which anodes were replaceable without disturbing the arrangement of the cathode and the membrane.

Anodes (DSAs®) of a louvered type (an assembled strip with a parallel array), a circularly perforated type and a mesh type were constructed as follows: a number of Ti strips 100 × (0.5 ~ 1.5) × (1.5 ~ 4) mm^3 were arranged in a louvered form so that they had an apparent area of 50 × 100 mm^2, and their ends were welded to two bus bars. A circularly perforated plate was constructed by punching a Ti plate (100 × 50 × (0.5 ~ 1.5) mm^3). The other geometry was a flattened mesh. Ti substrates with these three kinds of geometries were blasted, rinsed with water and then etched in 6 mol dm^{-3} HCl solution. They were soaked in HCl solution containing ruthenium chloride and titanium chloride, and were then baked in an oven at 400–500° C for 15 min in order to coat the Ti surface with RuO_2 and TiO_2. This process was repeated several times in order to obtain adequate catalyst layer thickness. Geometries of the DSA® anodes thus constructed are illustrated in Figs 2a–2c and their dimensions are listed in Tables 1–3 for the louvered electrodes, the circularly perforated plates and flattened meshes, respectively. The standard deviation of distances between two adjacent open parts was less than 0.05 mm. Resistance between a current feeder of the anode and the corner farthest from the feeder was

Table 1. Dimensions of louvered anodes and the cell voltage

Number of anodes	p_L (*mm*)	w_L (*mm*)	o_p (%)	t (*mm*)	$V - V_{rf}$ (V)
1	3.8	1.5	60	1.0	−0.06
2	3.0	1.5	50	1.0	−0.11
3	2.5	1.5	40	1.0	−0.08
4	2.1	1.5	30	1.0	−0.09
5	5.0	2.0	60	1.0	−0.07
6	4.0	2.0	50	1.0	−0.11
7	3.3	2.0	40	1.0	−0.11
8	2.9	2.0	30	1.0	−0.06
9	7.5	3.0	60	1.0	−0.01
10	6.0	3.0	50	1.0	−0.08
11	5.0	3.0	40	1.0	−0.08
12	4.3	3.0	30	1.0	−0.11
13	10.0	4.0	60	1.0	0.03
14	8.0	4.0	50	1.0	−0.00
15	6.7	4.0	40	1.0	−0.06
16	5.7	4.0	30	1.0	−0.10
17	3.0	1.5	50	1.5	−0.10
18	3.0	1.5	50	1.5	−0.11
19	4.0	2.0	50	0.5	−0.14
20	4.0	2.0	50	0.5	−0.11
21	4.0	2.0	50	0.5	−0.11

Table 2. Dimensions of circularly perforated anodes and the cell voltage

Number of anodes	p_{cp} (*mm*)	$2r$ (*mm*)	o_p (%)	t (*mm*)	$V - V_{rf}$ (V)
1	2.0	1.5	50	1.0	−0.15
2	2.3	1.5	40	1.0	−0.16
3	2.7	2.0	50	1.0	−0.15
4	3.0	2.0	40	1.0	−0.13
5	3.4	2.5	50	1.0	−0.15
6	3.8	2.5	40	1.0	−0.14
7	4.0	3.0	50	1.0	−0.13
8	4.5	3.0	40	1.0	−0.14
9	5.4	4.0	50	1.0	−0.12
10	6.0	4.0	40	1.0	−0.13
11	7.0	4.0	30	1.0	−0.09
12	8.0	6.0	50	1.0	−0.11
13	9.0	6.0	40	1.0	−0.10
14	10.5	6.0	30	1.0	−0.05
15	2.0	1.5	50	0.5	−0.18
16	4.0	3.0	50	0.5	−0.11
17	4.0	3.0	50	1.5	−0.10
18	8.0	6.0	50	0.5	−0.13
19	8.0	6.0	50	1.5	−0.13

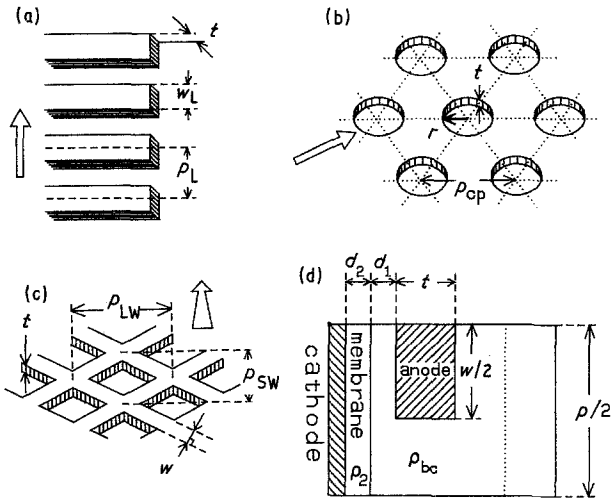

Fig. 2. Illustrations of (a) louvered (assembly of strip) electrodes; (b) circularly perforated electrodes; (c) flattened mesh electrodes; (d) two-dimensional rectangular model electrode. Bold arrows denote the vertical direction of anode configuration in the cell, i.e. the direction of the convection of electrolytes.

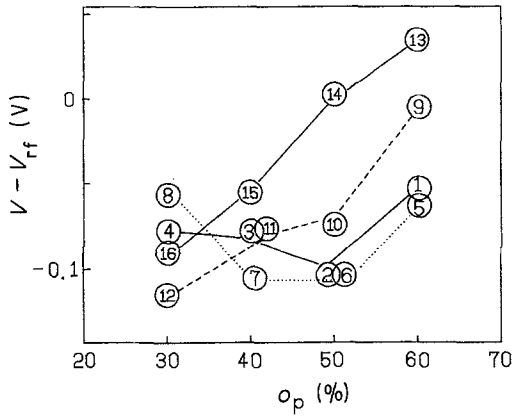

Fig. 3. Variations of $V - V_{rf}$ with o_p at the louvered electrodes. Numbers correspond to those in Table 1.

less than 5 mΩ. Thin meshes (Nos 1–6 in Table 3) were reinforced by large Ti meshes (12.7 × 6.35 mm^2) in order to maintain flatness.

A constant current was fed to the cell so that the apparent current density (the current divided by the apparent electrode area) was 0.3 A cm^{-2}. In this electrolysis, chlorine gas was generated at the anode and hydrogen gas at the cathode. The temperature in the cell was controlled at 90° C by a thermostat. The electrolytes, 3.5 mol dm^{-3} NaCl for an anolyte and 11 mol dm^{-3} NaOH for a catholyte, were supplied through inlet tubes (see Fig. 1) during electrolysis in order to maintain the concentrations. However, the flow of the electrolytes in the cell occurs mainly due to convection of solution caused by gas evolution.

The cell voltages at the DSA® after an hour's electrolysis were recorded through an electrometer HE105 (Hokuto Denko, Tokyo) for a few minutes with a pen recorder and were averaged.

Overpotentials at the anodes were measured with an automatic overpotential measurement system described previously [15], which was based on a current interrupter method. Overpotentials at 0.3 A cm^{-2} were less than 50 mV for all the DSAs® employed. They were much smaller than overall voltage, ca 3.5 V, indicating that the current distribution in the cell could be approximately considered as the primary current distribution.

3. Results and discussion

The cell model employed for the theoretical approach has been shown in Figs 3 and 4 of Ref. [3] or Fig. 2d, which is composed of an electrode with open parts and of the following three layers having different resistivity: a membrane, a bubble curtain and a convective layer. In the case of the primary current distribution, the cell voltage of the whole cell is given by the following approximate equation [1, 3]:

$$V = j[(\varrho_2 d_2 + \varrho_{bc} d_1) + 0.167(o_p/100)^{2.1}\varrho_{bc} p] + V_{rs} \quad (1)$$

Table 3. Dimensions of flattened mesh anodes and the cell voltage

Number of anodes	p_{LW} (*mm*)	p_{SW} (*mm*)	*w (strand) (mm)*	o_p (%)	*t (mm)*	$V - V_{rf}$ (*V*)
1	1.5	1.2	0.36	13	0.3	−0.06
2	2.0	1.4	0.36	32	0.3	−0.09
3	2.5	1.6	0.36	44	0.3	−0.09
4	3.0	1.8	0.48	37	0.4	−0.08
5	3.5	2.1	0.48	45	0.4	−0.06
6	4.5	2.7	0.48	56	0.4	−0.08
7	3.0	1.8	0.60	27	0.5	−0.08
8	4.5	2.7	0.60	41	0.5	−0.03
9	6.0	3.6	0.60	55	0.5	−0.03
10	4.5	2.7	0.90	10	0.75	0.00
11	6.0	3.6	0.90	40	0.75	−0.02
12	7.5	4.5	0.90	50	0.75	0.02
13	6.0	3.6	1.20	28	1.00	−0.01
14	7.5	4.5	1.20	37	1.00	−0.01
15	9.0	5.4	1.20	49	1.00	0.02
16	12.7	6.4	1.55	41	1.50	0.02

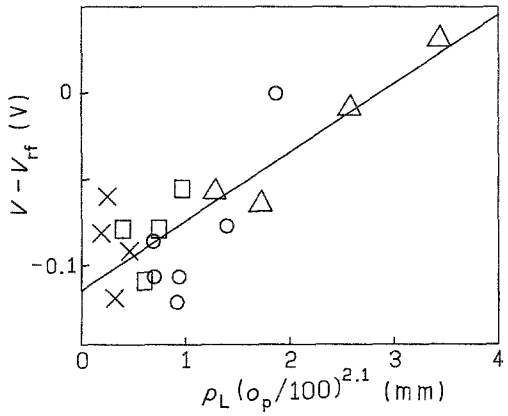

Fig. 4. Plots of $V - V_{rf}$ against $p_L(o_p/100)^{2.1}$ at the louvered electrodes for o_p = (△) 60, (○) 50, (□) 40 and (×) 30%.

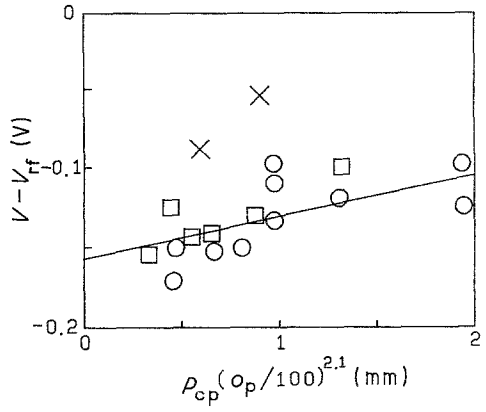

Fig. 5. Dependence of $V - V_{rf}$ on $p_{cp}(o_p/100)^{2.1}$ at the circularly perforated electrodes for o_p = (○) 50, (□) 40 and (×) 30%. The two crosses were neglected for drawing the straight line.

where o_p is the per cent open area given by

$$o_p = 100(p - w)/p \tag{2}$$

Equation 1 has been derived on the assumption that a value of ϱ_{bc} is constant over the bubble curtain. This assumption may be reasonable at the anode onto which the membrane is pressed, because the bubble curtain is probably saturated with bubbles in the vicinity of the membrane. If the membrane is mounted so far from the anode that bubbles are removed through the space, ϱ_{bc} cannot be regarded as constant. Then ϱ_{bc} might be a function of a distance from the anode [4–7, 9].

The first term of Equation 1 is composed of the resistance of the membrane, $j\varrho_2 d_2$, that of the bubble curtain, $j\varrho_{bc}d_1$, and the correlation term, $0.167j(o_p/100)^{2.1}\varrho_{bc}p$ depending on electrode geometries. It predicts that the cell voltage has a linear relation to p and $o_p^{2.1}$.

Since our concern is to specify effects of anode geometries on the cell voltage, it is desired to extract only the term $0.167j(o_p/100)^{2.1}\varrho_{bc}p$ from V, by subtracting V_{rs}. This requirement may be partly satisfied by finding a difference between the cell voltage for the anode of interest and that for an anode with a certain geometry. The latter anode is used as a reference for evaluating the difference in the voltages. The cell voltage in the cell with the latter anode, V_{rf}, is expressed by

$$V_{rf} = j\varrho_2 d_2 + V'_{rs} \tag{3}$$

where V'_{rs} involves not only V_{rs} but also geometrical effects of the reference anode. The difference between V and V_{rf} yields

$$V - V_{rf} = j[d_1 + 0.167(o_p/100)^{2.1}p]\varrho_{bc} + V_{rs} - V'_{rs} \tag{4}$$

$V - V_{rf}$ consists of the term depending on p and o_p and the terms independent of the anode geometries of interest. Thus variations of $V - V_{rf}$ with p and o_p may lead to separating the geometrical effect from V.

As the reference anode, a circularly perforated electrode similar to anode 4 in Table 2 was employed in all the series of measurements, being mounted in the cell 2 mm from the membrane. V_{rf} was measured before and after each measurement of V and it was confirmed that the two values of V_{rf} were the same within 0.03 V error. This procedure was repeated 2–4 times for measurements of $V - V_{rf}$ at each anode. When the differences in the two values were over 0.03 V, which may be ascribed to degradation of the cathodes and the membrane, the solution was renewed, and the cathodes and the membrane were rearranged in the cell.

The louvered electrode has the geometry closest to the model in Fig. 2d among the three types of anodes. The width of the strip, w_L, and a distance between two adjacent strips, p_L, obviously correspond to w and p of the model, respectively. In Fig. 3, the cell voltage, $V - V_{rf}$, measured at the louvered electrodes is plotted against o_p for several values of the width. The cell voltage increases with an increase in o_p when compared at the same value of w_L. This increase is ascribed to a decrease in the anode area facing the membrane. As values of w_L decrease at the same per cent open area, the cell voltage decreases for $o_p > 40\%$. This trend becomes weak for small values of o_p because a highly resistive bubble curtain is formed around the anode.

In Fig. 4, $V - V_{rf}$ at the louvered electrodes is plotted against $p(o_p/100)^{2.1}$. It is possible to draw a straight line on the plot although points exhibit appreciable scatter. The slope of the line is 0.4 V cm^{-1}, from which ϱ_{bc} is evaluated to be 8 Ω cm. This is four times as large as the resistivity of 3.5 mol dm^{-3} NaCl solution (approximately 2 Ω cm [5]), suggesting that a bubble curtain is present in the interelectrode and the open part regions.

For the circularly perforated anode, o_p is expressed by $o_p = (3^{1/2}\pi/6)(r/p_{cp})^2$. It is reasonable to regard p_{cp} as the pitch. In Fig. 5, variations of $V - V_{rf}$ measured at the circularly perforated anodes with $p_{cp}(o_p/100)^{2.1}$ are shown for three values of o_p. The plots except for those at $o_p = 30\%$ fall on a straight line, of which the slope is 0.2 V cm^{-1}, corresponding to $\varrho_{bc} = 4\,\Omega$ cm. This value is close to that obtained in the previous section. This analysis supports the validity of Equation 4 even for the circularly perforated electrode although Equation 4 has been derived on the basis of

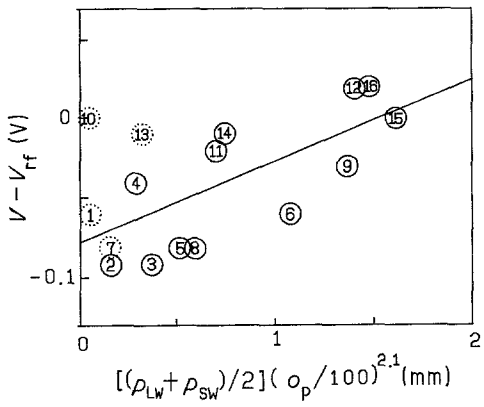

Fig. 6. Dependence of $V - V_{rf}$ on $[(p_{LW} + p_{SW})/2](o_p/100)^{2.1}$ at the flattened mesh electrodes. Numbers correspond to those in Table 3. The four dotted circles were neglected for drawing the straight line.

the two-dimensional rectangular model. The deviation of $V - V_{rf}$ at $o_p = 30\%$ from the line may be ascribed to slow removal of gas bubbles from the interelectrode region. In other words, ϱ_{bc} increases due to accumulation of gas bubbles at $o_p = 30\%$.

There was no dependence of $V - V_{rf}$ on thickness of the louvered and the circularly perforated anodes, as shown in Tables 1 and 2. This observation is in agreement with the previous theory [1].

It is expected that a plot similar to that in Fig. 5 may be effective for the voltage dependence on geometry of the flattened mesh anode. The per cent open area for the mesh electrode is formally expressed by

$$o_p = (p_{LW} - w/\sin\theta)(p_{SW} - w/\cos\theta)/(p_{LW}p_{SW}) \quad (5)$$

where $\theta = \arctan(p_{SW}/p_{LW})$. However, o_p in Table 3 was determined by measuring the ratio of the projected open area to the total area. The mesh electrode has basically two kinds of pitch, p_{LW} and p_{SW}, as shown in Fig. 2c. The plot may depend on which p is selected. In Fig. 6, the plot is shown when p is taken to be $(p_{LW} + p_{SW})/2$. Linear dependence is weak. However, if the data for $o_p < 30\%$, which gave large values of ϱ_{bc} at the circularly perforated anode, are excluded from the plot, a linear relation can be found and the slope gave $\varrho_{bc} = 10\,\Omega$cm. When p is taken to be p_{LW} and p_{SW}, a linear relation has also been observed and values of ϱ_{bc} are 12 and 8 Ωcm, respectively. Although there is ambiguous selection of p, Equation 4 holds also for the expanded-rolled mesh electrode for $o_p > 30\%$. The linearity is, however, worse than that for the louvered electrodes and the circularly perforated electrodes.

4. Conclusion

From the measurements of the cell voltages at anodes with various geometries, a small pitch and a small per cent open area reduced the cell voltage by a magnitude proportional to $o_p^{2.1}p$, as shown in Figs 4–6. This observation was supported by the theoretical evaluation of the current distribution in the two-dimensional rectangular model cell. A linear relation between the cell voltage and $o_p^{2.1}p$ was valid, not only for the louvered electrode, but also for the circularly perforated electrode with a three-dimensional configuration. Thus it is concluded that the approximate equation [4] derived with the two-dimensional model cell was valid for real three-dimensional anodes. For the flattened mesh, in which the pitch could not be determined unequivocally, the linear relation was weak. Slopes of the linear relation gave reasonable values of the solution resistivity increased by gas bubbles, which were a few times larger than the resistivity of the solution without gas bubles. This fact indicated formation of a bubble curtain around the anode. Too small a per cent open area ($o_p < 30\%$), however, increased the cell voltage because of pronounced accumulation of gas bubbles. Thus, there was an optimum range of the per cent open area around 40%.

References

[1] Y. Nishiki, K. Aoki, K. Tokuda and H. Matsuda, *J. Appl. Electrochem.* **14** (1984) 653.
[2] Y. Nishiki, K. Aoki, K. Tokuda and H. Matsuda, *J. Appl. Electrochem.* **16** (1986) 291.
[3] Y. Nishiki, K. Aoki, K. Tokuda and H. Matsuda, *J. Appl. Electrochem.* **17** (1987) 67.
[4] L. E. Vaaler, *J. Appl. Electrochem.* **9** (1978) 21.
[5] J. Jorne and J. F. Louvar, *J. Electrochem. Soc.* **127** (1980) 298.
[6] F. Hine, M. Yasuda, M. Watanabe and M. Kurata, *Soda to Enso* (*Soda and Chlorine*) **7** (1981) 281.
[7] F. Hine and K. Murakami, *J. Electrochem. Soc.* **128** (1981) 64.
[8] L. J. J. Janssen, J. J. M. Geraets, E. Barendrecht and S. D. J. Van Stralen, *Electrochim. Acta* **27** (1982) 1207.
[9] F. Hine, M. Tasuda, Y. Ogata and K. Hara, *J. Electrochem. Soc.* **131** (1984) 83.
[10] C. Elsner and F. Coeuret, *J. Appl. Electrochem.* **15** (1985) 567.
[11] Y. Nishiki, K. Aoki, K. Tokuda and H. Matsuda, *J. Appl. Electrochem.* **17** (1987) 445.
[12] K. Aoki, Y. Nishiki, K. Tokuda and H. Matsuda, *J. Appl. Electrochem.* **17** (1987) 552.
[13] R. J. Horvath, in 'Modern Chlor-Alkali Technology' (edited by K. Wall), Ellis Horwood, New York (1986) Vol. 3, Ch. 17.
[14] O. Lanzi, R. F. Savinell and R. E. Horn, *J. Appl. Electrochem.* **14** (1984) 425.
[15] K. Aoki, Y. Nishiki, K. Tokuda and H. Matsuda, *Denkikagaku* (*J. Electrochem. Soc. Jpn*) **55**, (1987) 34.